

On the Theoretical Foundation of Sparse Dictionary Learning in Mechanistic Interpretability

Yiming Tang¹ Harshvardhan Saini² Zhaoqian Yao³ Yizhen Liao¹ Qianxiao Li¹ Mengnan Du⁴ Dianbo Liu¹

Abstract

As AI models achieve remarkable capabilities across diverse domains, understanding what representations they learn and how they process information has become increasingly important for both scientific progress and trustworthy deployment. Recent works in mechanistic interpretability have shown that neural networks represent meaningful concepts as directions in their representation spaces and often encode diverse concepts in superposition. Various sparse dictionary learning (SDL) methods, including sparse autoencoders, transcoders, and crosscoders, address this by training auxiliary models with sparsity constraints to disentangle these superposed concepts into monosemantic features. These methods have demonstrated remarkable empirical success but have limited theoretical understanding. Existing theoretical work is limited to sparse autoencoders with tied-weight constraints, leaving the broader family of SDL methods without formal grounding. In this work, we develop the first unified theoretical framework considering SDL as one optimization problem. We demonstrate how diverse methods instantiate the theoretical framework and provide rigorous analysis of the optimization landscape. We provide novel theoretical explanations for empirically observed phenomena, including feature absorption and dead neurons. We design the Linear Representation Bench, a benchmark that strictly follows the Linear Representation Hypothesis, to evaluate SDL methods with fully accessible ground-truth features. Motivated by our theory and findings, we develop feature anchoring, a novel technique applicable for all SDL methods, to enhance their feature recovery capabilities.

1. Introduction

As artificial intelligence is increasingly deployed in high-stakes applications, from medical diagnosis to autonomous systems, the need for model interpretability has grown from an academic curiosity to a practical necessity (Lipton, 2017; Rudin, 2019). Numerous approaches have been proposed to peer inside the “black box,” including probing classifiers (Belinkov, 2021), attention visualization (Vaswani et al., 2023), concept bottleneck models (Koh et al., 2020), and feature attribution methods (Sundararajan et al., 2017). Among the efforts to enhance model interpretability, one line of research focuses on the structure of the model representations, pointing out that AI models often encode interpretable concepts as linear directions in superposition (Park et al., 2024; Elhage et al., 2022). As a consequence, individual neurons are typically polysemantic, responding to multiple unrelated concepts unlike their biological counterparts (Bricken et al., 2023; Templeton et al., 2024; Quiroga et al., 2005).

To address the polysemantic model representations, Sparse Dictionary Learning (SDL) has emerged as a promising paradigm (Sharkey et al., 2025). By training auxiliary models, such as sparse autoencoders (SAEs) (Cunningham et al., 2023), transcoders (Dunefsky et al., 2024), and crosscoders (Lindsey et al., 2024), that reconstruct neural activations through a sparsity-constrained bottleneck, SDL methods aim to identify the interpretable concepts underlying the polysemantic representations. These methods have achieved remarkable empirical success, scaling to frontier language models (Templeton et al., 2024; Gao et al., 2024) and enabling applications ranging from feature steering (Wang et al., 2025) to circuit analysis (O’Neill & Bui, 2024) and interpretable medical diagnosis (Abdulaal et al., 2024).

Despite these empirical advances, due to a lack of unified theoretical framework to analyze SDL methods, the field identifies various phenomena without rigorous theoretical explanation, including feature splitting and feature absorption (Chanin et al., 2025), the existence of dead neurons and the effectiveness of resampling (Bricken et al., 2023). Without theoretical grounding, the development of improved SDL methods remains largely empirical, potentially leaving highly effective techniques underexplored. While previous works on sparse coding and dictionary learning have es-

¹National University of Singapore ²Indian Institute of Technology ³Chinese University of Hong Kong ⁴New Jersey Institute of Technology. Correspondence to: Yiming Tang <yiming@nus.edu.sg>, Dianbo Liu <dianbo@nus.edu.sg>.

tablished solid theoretical results (Spielman et al., 2012; Gribonval & Schnass, 2010), these results do not directly address SDL methods used in mechanistic interpretability. Recent work by Cui et al. (2025) has taken a key step by establishing necessary and sufficient conditions for identifiable sparse autoencoders under the linear representation hypothesis. However, their framework focuses exclusively on SAEs with tied-weight constraints, leaving other SDL methods without theoretical grounding.

In this work, we develop a unified theoretical framework that formalizes SDL as a general optimization problem, encompassing various SDL methods (Bussmann et al., 2024; 2025; Tang et al., 2025b) as special cases. We demonstrate how these diverse methods instantiate our framework through different choices of input-output representation pairs, activation functions, and loss designs. We establish rigorous conditions under which SDL methods provably recover ground-truth interpretable features, characterizing the roles of feature sparsity, latent dimensionality, and activation functions. Through detailed analysis of the optimization landscape, we demonstrate that global minima correspond to correct feature recovery while spurious local minima exhibit un-disentangled polysemanticity, providing novel theoretical explanation for feature absorption (Chanin et al., 2025) and neuron resampling (Bricken et al., 2023). We design the Linear Representation Bench, a synthetic benchmark that strictly follows the Linear Representation Hypothesis, to evaluate SDL methods with fully accessible ground-truth features. Motivated by our theoretical insights, we propose feature anchoring that achieve improved feature recovery by constraining learned features to known anchor directions. Our contributions are as follows:

- We build the first theoretical framework for SDL in mechanistic interpretability as a general optimization problem encompassing diverse SDL methods.
- We provide rigorous theoretical results on the optimization landscape and provide novel explanations for various phenomena observed empirically.
- We design the Linear Representation Bench, a benchmark enabling controlled evaluation of SDL methods with fully accessible ground-truth features.
- We propose feature anchoring that constrains learned features to known anchor directions, achieving improved feature recovery performance.

2. Preliminaries

In this section, we present a unified theoretical framework for Sparse Dictionary Learning (SDL). We begin with the formal definitions of foundational concepts and the linear

representation hypothesis. Then we introduce our framework and how various SDL methods instantiate it.

2.1. Input Distribution and Model Representation

Definition 2.1 (Input Distribution). Let \mathcal{D} denote the distribution over possible inputs to a neural network. For example, \mathcal{D} could be the distribution of natural images or the distribution of text sequences.

Definition 2.2 (Model Representation). For a given model representation \mathbf{x} , let $n \in \mathbb{N}$ be its dimensionality. For each $s \sim \mathcal{D}$, the network produces a representation vector $\mathbf{x}(s)$, which is directly observable by running the model on s .

2.2. The Linear Representation Hypothesis

Empirical studies in mechanistic interpretability have observed that neural network representations encode meaningful concepts as linear directions, often in superposition (Marks & Tegmark, 2024; Nanda et al., 2023; Jiang et al., 2024; Park et al., 2025). Following Elhage et al. (2022) and Park et al. (2024), we formalize the hypothesis as follows.

Assumption 2.3 (Linear Representation Hypothesis). A model representation $\mathbf{x}_p \in \mathbb{R}^{n_p}$ satisfies the Linear Representation Hypothesis (LRH) if there exists a *feature function* $\mathbf{x} : \mathcal{D} \rightarrow \mathbb{R}^n$ and a *feature matrix* $W_p \in \mathbb{R}^{n_p \times n}$ such that:

1. **Linear Decomposition:** For all $s \sim \mathcal{D}$,

$$\mathbf{x}_p(s) = W_p \mathbf{x}(s).$$

2. **Non-negativity:** $\mathbf{x}(s) \geq 0$ component-wise.

3. **Sparsity:** There exists $S \in [0, 1]$ such that $\forall i \in [n]$,

$$\Pr_{s \sim \mathcal{D}} (x_i(s) = 0) \geq S.$$

4. **Interpretability:** Each component x_i of \mathbf{x} corresponds to a human-interpretable concept.

We refer to $\mathbf{x}(s)$ as the *ground-truth features*, where each $x_i(s)$ represents the activation level of concept i for input s . W_p encodes how these features are represented in \mathbf{x}_p .

Assumption 2.4 (Representation Assumptions). Following recent works (Elhage et al., 2022; Park et al., 2024), we assume the following conditions on the model representations satisfying the Linear Representation Hypothesis, which align with practical use cases:

1. **Unit Norm:** The feature matrix $W_p \in \mathbb{R}^{n_p \times n}$ has unit-norm columns:

$$\|W_p[:, i]\|_2 = 1 \quad \forall i \in [n]$$

2. **Bounded Interference:** Define the *maximum interference* as:

$$M := \max_{i \neq j} \langle W_p[:, i], W_p[:, j] \rangle$$

In typical superposition scenarios, $M > 0$ but remains small (close to zero), characterizing a regime where many interpretable features are compressed into fewer dimensions with bounded mutual interference.

3. **Extreme Sparsity:** The sparsity level S approaches 1:

$$S \rightarrow 1$$

4. **Independence:** The ground-truth features satisfy: For any input $s \sim \mathcal{D}$, the features $\{x_i(s)\}_{i=1}^n$ are mutually independent and independent of the sparsity level S .

where $W_p[:, i]$ denotes the i -th column of W_p .

2.3. General Optimization Framework for SDL

Now we formalize SDL as an optimization problem under the Linear Representation Hypothesis (Assumption 2.3) and the Representation Assumptions (Assumption 2.4).

Definition 2.5 (Sparse Dictionary Learning). A SDL model maps an input representation $\mathbf{x}_p \in \mathbb{R}^{n_p}$ to a target representation $\mathbf{x}_r \in \mathbb{R}^{n_r}$ through a two-layer architecture:

(i) An *encoder* layer that maps \mathbf{x}_p to a latent space:

$$\mathbf{x}_q = \sigma(W_e \mathbf{x}_p) \quad (1)$$

(ii) A *decoder* layer that maps the latents to \mathbf{x}_r :

$$\hat{\mathbf{x}}_r = W_d \mathbf{x}_q \quad (2)$$

where $\mathbf{x}_q \in \mathbb{R}^{n_q}$, $W_e \in \mathbb{R}^{n_q \times n_p}$, $W_d \in \mathbb{R}^{n_r \times n_q}$, and $\sigma : \mathbb{R}^{n_q} \rightarrow \mathbb{R}^{n_q}$ is a sparsity-inducing activation function.

The SDL objective minimizes expected reconstruction error:

$$\mathcal{L}_{\text{SDL}} = \mathbb{E}_{s \sim \mathcal{D}} [\|\mathbf{x}_r(s) - W_d \sigma(W_e \mathbf{x}_p(s))\|_2^2] \quad (3)$$

Under the Linear Representation Hypothesis (Assumption 2.3), both representations admit linear decompositions $\mathbf{x}_p(s) = W_p \mathbf{x}(s)$ and $\mathbf{x}_r(s) = W_r \mathbf{x}(s)$ in terms of ground-truth features $\mathbf{x}(s)$. The loss can thus be expressed as:

$$\mathcal{L}_{\text{SDL}} = \mathbb{E}_{s \sim \mathcal{D}} [\|W_r \mathbf{x}(s) - W_d \sigma(W_e W_p \mathbf{x}(s))\|_2^2] \quad (4)$$

2.4. Instantiations: Existing SDL Methods

We now demonstrate how existing SDL methods instantiate our framework through adopting different choices of

input-target pairs $(\mathbf{x}_p, \mathbf{x}_r)$ and activation functions σ , and proposing variants on the loss function \mathcal{L}_{SDL} .

Sparse Autoencoders (SAEs). SAEs (Cunningham et al., 2023) decompose polysemantic activations into monosemantic components through sparsity constraints. In our framework, SAEs are characterized by setting $\mathbf{x}_r = \mathbf{x}_p$ (self-reconstruction). The encoder projects to a higher-dimensional sparse latent space, encouraging $\mathbf{x}_q(s)$ to capture the underlying ground-truth features $\mathbf{x}(s)$ (Figure 1).

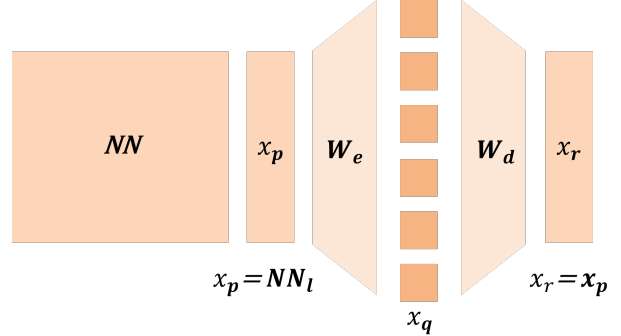


Figure 1. Sparse Autoencoder: encoder W_e maps \mathbf{x}_p to sparse latents \mathbf{x}_q , decoder W_d reconstructs from \mathbf{x}_q .

Transcoders. Transcoders (Dunefsky et al., 2024; Paulo et al., 2025) capture interpretable features in layer-to-layer transformations. Unlike SAEs, transcoders approximate the inputoutput function of a target component, such as an MLP, using a sparse bottleneck. In our proposed theoretical framework, transcoders set $\mathbf{x}_p = \text{NN}_\ell(s)$ and $\mathbf{x}_r = \text{NN}_{\ell+1}(s)$, where NN_ℓ denotes the target component's input, and $\text{NN}_{\ell+1}$ denotes its output (Figure 2).

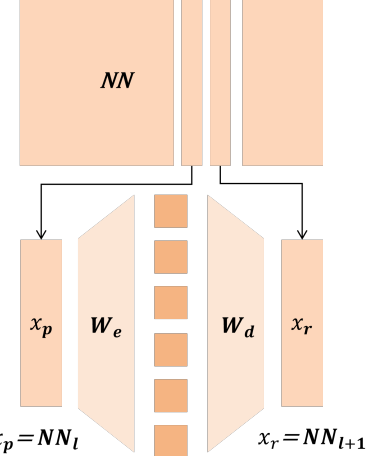


Figure 2. Transcoder: encoder W_e maps $\text{NN}_\ell(s)$ to sparse latents \mathbf{x}_q , decoder W_d predicts $\text{NN}_{\ell+1}(s)$.

Crosscoders. Crosscoders (Lindsey et al., 2024) discover shared features across multiple representation sources

by jointly encoding and reconstructing concatenated representations. In our framework, crosscoders set $\mathbf{x}_p = [\mathbf{x}_p^{(1)}; \dots; \mathbf{x}_p^{(m)}]$ and $\mathbf{x}_r = [\mathbf{x}_r^{(1)}; \dots; \mathbf{x}_r^{(m)}]$ where each superscript denotes a different source (Figure 3).

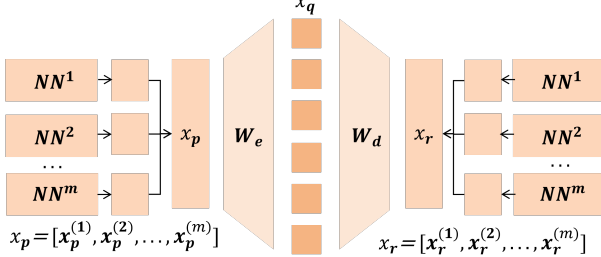


Figure 3. Crosscoder: encoder W_e maps concatenated multi-layer input \mathbf{x}_p to \mathbf{x}_q , decoder W_d reconstructs multi-layer output \mathbf{x}_r .

Variants of SDL Methods. Various SDL methods fit into our theoretical framework but differ in their choices of activation functions and loss designs. Bricken et al. (2023) and Templeton et al. (2024) use ReLU activation $\sigma_{\text{ReLU}}(z) = \max(0, z)$ with L_1 regularization on latents:

$$\mathcal{L} = \mathbb{E}_{s \sim \mathcal{D}} [\|\mathbf{x}_r(s) - W_d \sigma_{\text{ReLU}}(W_e \mathbf{x}_p(s))\|_2^2 + \lambda \|\mathbf{x}_q(s)\|_1] \quad (5)$$

Rajamanoharan et al. (2024b) propose to utilize JumpReLU as the activation function:

$$\sigma_{\text{JumpReLU}}(z) = z \cdot H(z - \theta) \quad (6)$$

combined with a smoothed Heaviside function to directly penalize the L_0 norm. Makhzani & Frey (2014) introduce Top- k activation:

$$\sigma_{\text{Top-}k}(z)_i = \begin{cases} z_i & \text{if } z_i \text{ is among the } k \text{ largest components} \\ 0 & \text{otherwise} \end{cases} \quad (7)$$

Bussmann et al. (2024) extend this to Batch Top- k activation, which applies Top- k selection across a batch to allow different samples to have different numbers of activated features. Rajamanoharan et al. (2024a) use ReLU activation with an additional Heaviside gating function. Gao et al. (2024) employ Top- k activation and introduce an auxiliary loss using Top- k_{aux} dead latents:

$$\begin{aligned} \mathcal{L} = \mathbb{E}_{s \sim \mathcal{D}} & [\|\mathbf{x}_r(s) - W_d \sigma_{\text{Top-}k}(W_e \mathbf{x}_p(s))\|_2^2 \\ & + \lambda_{\text{aux}} \|\mathbf{x}_p(s) - W'_d \sigma_{\text{Top-}k_{\text{aux}}}(W_e \mathbf{x}_p(s))\|_2^2] \end{aligned} \quad (8)$$

to resurrect dead neurons. Bussmann et al. (2025) and Tang et al. (2025b) use multiple k values with a multi-scale loss:

$$\mathcal{L} = \sum_{i=1}^m \lambda_i \mathbb{E}_{s \sim \mathcal{D}} [\|\mathbf{x}_r(s) - W_d \sigma_{\text{Top-}k_i}(W_e \mathbf{x}_p(s))\|_2^2] \quad (9)$$

that sums reconstruction errors of different sparsity levels.

The variants described above demonstrate that diverse SDL methods can be unified under our general framework (Definition 2.5) through specific choices of activation functions σ and loss modifications. This motivates our theoretical approach: rather than analyzing each variant separately, we establish a key property for all these activation functions.

Key Activation Function Property. Our analysis focuses on activation functions satisfying:

$$\sigma(z)_i \in \{0, z_i\} \quad \forall i \in [n_q] \quad (10)$$

This property holds for ReLU, JumpReLU, Top- k , Batch Top- k , and their compositions, the primary sparsity mechanisms in practice. Notably, all these activation functions can be expressed in the form $\sigma_{\text{Jump}}(z; c)$ for some threshold $c \geq 0$:

$$\sigma_{\text{Jump}}(z; c)_i = z_i \cdot \mathbb{1}(z_i > c) \quad (11)$$

3. Theoretical Results

Despite the empirical success of SDL methods across diverse applications, a significant gap exists between their practical use and our theoretical understanding of their optimization dynamics. This gap has important consequences: practitioners employ techniques like dead neuron resampling (Bricken et al., 2023) and observe phenomena like feature absorption (Chanin et al., 2025) without rigorous explanations for why these occur or how to systematically address them. Without theoretical grounding, the development of improved SDL methods remains largely empirical, potentially leaving highly effective techniques underexplored.

Our theoretical analysis bridges this gap by characterizing the SDL optimization landscape under the Linear Representation Hypothesis. Section 3.1 derives the necessary and sufficient conditions for the global minima of the optimization problem. Section 3.2 demonstrates the existence of spurious local minima and how they relate with polysemaniticity. Section 3.3 discusses about feature absorption and hierarchical concepts. We provide full proofs in Appendix.

3.1. Global Minimum

Here we analyze the global minima of our proposed framework. Theorem 3.1 shows that \mathcal{L}_{SDL} is well-approximated by an alternative loss on feature reconstructions, $\tilde{\mathcal{L}}_{\text{SDL}}$.

Theorem 3.1 (Loss Approximation). *Under Assumption 2.3 and Assumption 2.4, define the approximate Loss, $\tilde{\mathcal{L}}_{\text{SDL}}$, as:*

$$\tilde{\mathcal{L}}_{\text{SDL}}(W_d, W_e) := \sum_{d=1}^n M_d \|w_r^d - W_d \sigma(W_e w_p^d)\|^2 \quad (12)$$

where $M_d = \Pr(\mathbf{x}(s) = x_d(s)e_d) \cdot \mathbb{E}[x_d(s)^2 | x_d(s) > 0]$.

Then

$$|\mathcal{L}_{SDL} - \tilde{\mathcal{L}}_{SDL}| \leq O((1-S)^2) \quad (13)$$

Theorem 3.2 then demonstrates that the configuration $(W_d^*, W_e^*) = ([W_r, \mathbf{0}], [W_p^\top; \mathbf{0}])$ achieves approximate loss bounded by $O((1-S)M^2)$, establishing it as a near-optimal solution that recovers the ground-truth feature structure.

Theorem 3.2 (Approximate Loss at Global Minimum Configuration). *Consider the approximate SDL loss*

$$\tilde{\mathcal{L}}_{SDL}(W_d, W_e) = \sum_{d=1}^n M_d \|w_r^d - W_d \sigma(W_e w_p^d)\|^2 \quad (14)$$

where $M_d = \Pr(\mathbf{x}(s) = x_d(s)e_d) \cdot \mathbb{E}[x_d(s)^2 | x_d(s) > 0]$.

When $n_q \geq n$ and σ satisfies $\sigma(z)_i \in \{0, z_i\}$ for all i , the configuration

$$W_d^* = [W_r, \mathbf{0}], \quad W_e^* = \begin{bmatrix} W_p^\top \\ \mathbf{0} \end{bmatrix} \quad (15)$$

where $\mathbf{0}$ denotes zero padding to dimension n_q , satisfies:

$$\tilde{\mathcal{L}}_{SDL}(W_d^*, W_e^*) = O((1-S)M^2) \quad (16)$$

where M is the maximum interference.

Notice that the necessary and sufficient conditions for $\tilde{\mathcal{L}}_{SDL} = 0$ require $w_r^d = W_d \sigma(W_e w_p^d)$ for all $d \in [n]$. This system of n vector equations in the encoder-decoder parameters is underdetermined, admitting multiple solutions beyond (W_d^*, W_e^*) . Crucially, some solutions achieve zero reconstruction loss without recovering any ground-truth features, as demonstrated in Figure 4. This underdetermined nature motivates feature anchoring, a novel technique that applies additional constraints to guide optimization.

3.2. Polysemanticity and Local Minima

We now establish that SDL optimization can converge to spurious local minima with loss strictly greater than the global optimum. We also point out the connection between local minima and un-disentangled polysemanticity.

Example 3.3 (Spurious Local Minimum). Consider $n = n_p = n_q = n_r = 2$, $\sigma = \sigma_{\text{Top-1}} \cdot \sigma_{\text{ReLU}}$, and extreme sparsity ($S \rightarrow 1$). Let $W_e = \begin{bmatrix} (w_e^1)^\top \\ (w_e^2)^\top \end{bmatrix}$ and $W_d = [w_d^1, w_d^2]$. The approximate loss decomposes as:

$$\begin{aligned} \tilde{\mathcal{L}}_{SDL}(W_d, W_e) = & M_1 \|w_r^1 - W_d \sigma(W_e w_p^1)\|^2 \\ & + M_2 \|w_r^2 - W_d \sigma(W_e w_p^2)\|^2 \end{aligned} \quad (17)$$

where $M_1, M_2 > 0$ are constants.

Consider a configuration where:

$$\langle w_e^1, w_p^1 \rangle > \langle w_e^2, w_p^1 \rangle > 0, \quad \langle w_e^1, w_p^2 \rangle > \langle w_e^2, w_p^2 \rangle > 0 \quad (18)$$

Under this condition, neuron 1 activates for both features while neuron 2 remains dead. Let $a_1 = \langle w_e^1, w_p^1 \rangle$ and $a_2 = \langle w_e^1, w_p^2 \rangle$. The optimal decoder is:

$$w_d^{1,*} = \frac{M_1 a_1 w_r^1 + M_2 a_2 w_r^2}{M_1 a_1^2 + M_2 a_2^2} \quad (19)$$

Since $w_r^1 \not\propto w_r^2$, the resulting loss is:

$$\tilde{\mathcal{L}}_{SDL}^* = \frac{M_1 M_2 (M_2 a_2^2 + M_1 a_1^2) \|a_2 w_r^1 - a_1 w_r^2\|^2}{(M_1 a_1^2 + M_2 a_2^2)^2} > 0 \quad (20)$$

The spurious local minimum in Example 3.3 demonstrates a prevalent failure mode for SDL methods: a single SDL latent neuron becomes polysemantic, responding to multiple ground-truth features, while other neurons remain dead. This occurs when optimization becomes trapped in a local minimum where gradient descent cannot escape. We now formalize and characterize this polysemanticity.

Definition 3.4 (Polysemanticity Pattern). A *polysemanticity pattern* is a collection $(\mathcal{F}_1, \dots, \mathcal{F}_{n_q})$ where each $\mathcal{F}_i \subseteq [n]$ represents a subset of ground-truth features. The pattern is called *polysemantic* if $\exists i, |\mathcal{F}_i| \geq 2$.

Given an SDL configuration with activation function σ and projection vectors $\{w_p^d\}_{d=1}^n$, a polysemanticity pattern $(\mathcal{F}_1, \dots, \mathcal{F}_{n_q})$ forming a partition of $[n]$ is called *realizable* if there exists an encoder $W_e = [(w_e^1)^\top, \dots, (w_e^{n_q})^\top]^\top$ such that:

$$\forall i \in [n_q], \quad \mathcal{F}_i = \left\{ d \in [n] : (\sigma(W_e w_p^d))_i > 0 \right\} \quad (21)$$

That is, neuron i activates for exactly the features in \mathcal{F}_i when they are active in isolation.

Theorem 3.5 (Existence of Spurious Local Minima). Consider $\tilde{\mathcal{L}}_{SDL}(W_d, W_e) = \sum_{d=1}^n M_d \|w_r^d - W_d \sigma(W_e w_p^d)\|^2$ under Assumptions 2.3 and 2.4 with $n \geq 2$ and $n_q \geq n$.

For any realizable polysemanticity pattern $(\mathcal{F}_1, \dots, \mathcal{F}_{n_q})$ with at least one $|\mathcal{F}_i| \geq 2$, there exists a local minimum point (W_d, W_e) of the framework exhibiting this pattern.

3.3. Feature Absorption and Hierarchical Concepts

Empirical observations suggest that feature absorption is prevalent during the training of SDL (Chanin et al., 2025). We argue that this phenomenon arises when ground-truth features exhibit *hierarchical structure* and can be considered as a special type of realizable polysemanticity pattern.

Example 3.6 (Feature Absorption). Consider a representation space containing animal concepts. Ground-truth features include a parent concept "Dog" and four sub-concepts: "Border Collie", "Golden Retriever", "Husky", and "German Shepherd".

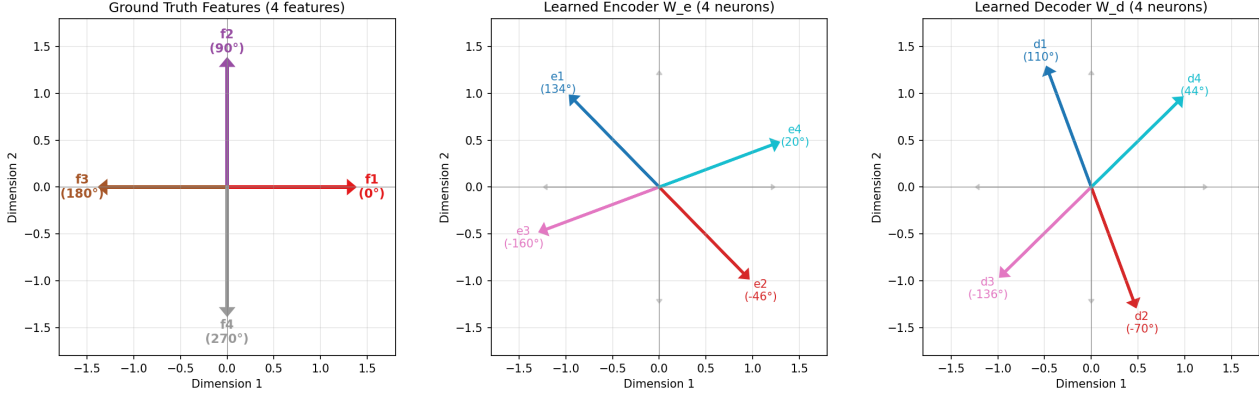


Figure 4. Zero reconstruction loss without recovering ground-truth features. We design the Linear Representation Bench that enable full knowledge of the ground truth features to study SDL methods. We observe one concerning phenomenon that these methods can achieve zero loss without recovering any ground truth features. **Left:** Four ground-truth feature directions. **Middle:** Learned encoder directions fail to align with ground truth. **Right:** Learned decoder directions are rotated accordingly. Although $\mathcal{L}_{SDL} \approx 0$, the learned features bear no correspondence to interpretable ground-truth concepts, demonstrating the underdetermined nature of SDL optimization.

As illustrated in Figure 5, in the ideal case, SDL would learn four separate monosemantic neurons for Dog, Cat, Horse, and Elephant, with each dog breed activating only the Dog neuron. However, feature absorption can occur during training, resulting in the pattern shown in Figure 5 (right): one neuron exclusively captures "Border Collie" (the absorbed feature), while a second neuron responds to the remaining three breeds collectively (the main line interpretation of "Dog").

Definition 3.7 (Hierarchical Concept Structure). A set of ground-truth features exhibits hierarchical structure if it contains a p and a set of *sub-concepts* c_1, \dots, c_k satisfying: $p(x) > 0 \iff \exists i \in [k], c_i(x) > 0$.

Theorem 3.8 (Existence of Feature Absorption). Any ground truth features exhibiting hierarchical structure correspond to a polysemy pattern with feature absorption. If realizable, there is a local minimum point exhibiting it.

Theorem 3.5 reveals the prevalence of local minima in SDL training that challenge gradient-based optimization and their connection to polysemant neurons. Theorem 3.8 shows that hierarchical concept structures naturally give rise to feature absorption patterns, which manifest as local minima when realizable, explaining its empirical prevalence.

4. The Feature Anchoring

Motivated by our theoretical results, we propose Anchored Sparse Autoencoders (See Figure 6) to guide optimization toward the global optimum. Specifically, we constrain the first k encoder rows and decoder columns to match ground-truth feature directions via an auxiliary loss to mitigate the

undetermined nature of the SDL optimization problem:

$$\mathcal{L}_{\text{anchor}} = \|\mathbf{W}_e[1:k, :] - \tilde{\mathbf{W}}_p[:, 1:k]^T\|_F^2 + \|\mathbf{W}_d[:, 1:k] - \tilde{\mathbf{W}}_r[:, 1:k]\|_F^2 \quad (22)$$

These anchor features are obtained either from ground-truth when available (Linear Representation Bench) or by computing mean embeddings of dataset subpopulations (Luo et al., 2024). During the evaluation, we only compute the recovery metric for features that were not selected as anchors.

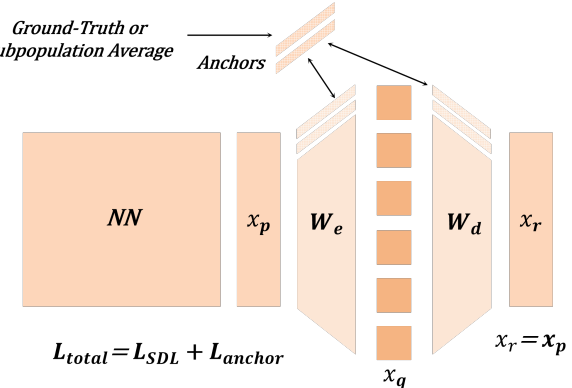


Figure 6. Anchored SAE. First k neurons (highlighted) constrained to ground-truth via $\mathcal{L}_{\text{anchor}}$; other neurons learn via SDL.

5. Experimental Results

5.1. The Linear Representation Bench

To validate our theoretical predictions, we design the Linear Representation Bench, a benchmark that precisely instantiates Assumptions 2.3 and 2.4. We generate synthetic representations $\mathbf{x}_p(s) = \mathbf{W}_p \mathbf{x}(s)$ where ground-truth features

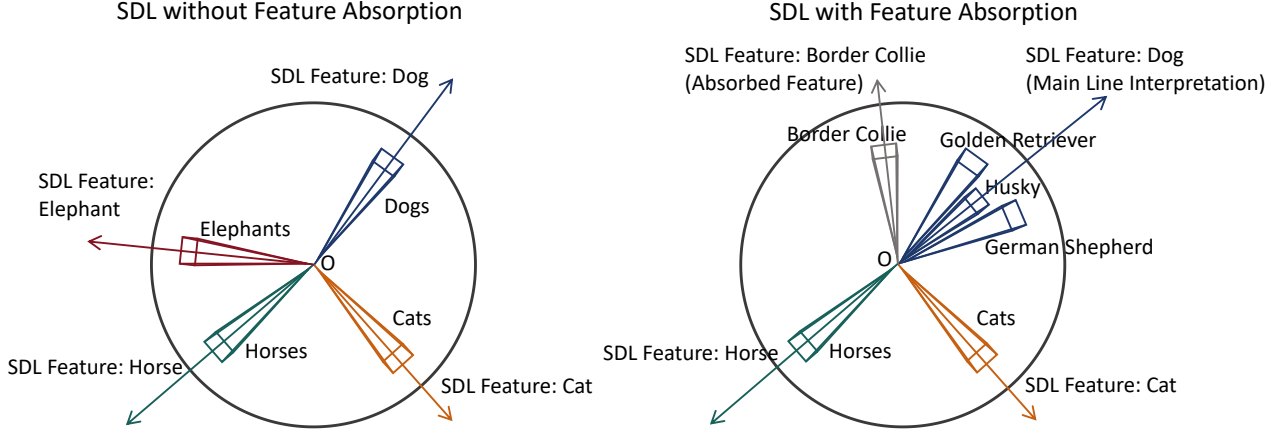


Figure 5. Feature absorption emerges from hierarchical concept structure. Left: Ideal SDL features without absorption. Right: hierarchical concept structure exists and only a proportion of the sub-concepts of "Dog" can activate the SDL feature.

$\mathbf{x}(s) \in \mathbb{R}^n$ follow shifted exponential distributions with sparsity \mathcal{S} . The feature matrix $\mathbf{W}_p \in \mathbb{R}^{n_p \times n}$ is constructed via gradient-based optimization to satisfy bounded interference $|\langle \mathbf{w}_p^i, \mathbf{w}_p^j \rangle| \leq \epsilon$ or negative interference $\langle \mathbf{w}_p^i, \mathbf{w}_p^j \rangle \leq 0$ with unit-norm columns. We evaluate SDL methods by measuring feature recovery: $\mathbb{E}_i[\max_j |\langle \mathbf{w}_p^i, \mathbf{w}_e^j \rangle|]$, the expected maximum alignment between each ground-truth feature \mathbf{w}_p^i and learned encoder columns \mathbf{w}_e^j . As shown in Table 1, our proposed Anchored SAE significantly improves feature recovery performance.

Interference	n	Method	
		SAE	Anchored SAE
Bounded	1000	0.256	0.284
Negative	1000	0.235	0.260

Table 1. We compare standard SAE and Anchored SAE (with $k = 30$ anchor features) on synthetic representations in $d = 768$ dimensions with $n \in \{1000, 1500, 2000\}$ features (Appendix C).

5.2. Neuron Resampling Helps Escape Local Minima

Our local minima analysis (Theorem 3.5) provides a novel explanation for why dead neuron resampling (Bricken et al., 2023) improves SDL training. Dead neurons ($\mathcal{F}_i = \emptyset$) contribute zero gradient in spurious local minima, leaving optimization trapped. Resampling reinitializes these neurons toward under-reconstructed directions, perturbing the optimization away from the local basin. To validate this, we conduct experiments on the Llama 3 model (Figure 7). Resampling enables the optimizer to escape spurious local minima, achieving lower reconstruction loss.



Figure 7. Feature resampling accelerates convergence and improves final loss. Training curves on Llama 3 comparing standard SAE training (blue) with periodic dead neuron resampling (red).

6. Related Works

6.1. Mechanistic Interpretability

Interpretability is crucial for deploying AI in high-stakes domains such as medical diagnosis and financial modeling, where understanding model decisions is essential for safety and trust (Simon & Zou, 2024; Abdulaal et al., 2024). Traditional approaches include interpretability-by-design methods like Concept Bottleneck Models (Koh et al., 2020) and decision trees (Mienye & Jere, 2024), and post-hoc explanation methods like GradCAM (Selvaraju et al., 2019) and SHAP (Lundberg & Lee, 2017). Mechanistic interpretability (Sharkey et al., 2025; Bereska & Gavves, 2024) aims to reverse-engineer neural networks by understanding their internal computational mechanisms. SAEs (Shu et al., 2025) and related dictionary learning methods (Tang et al., 2025a; Dunefsky et al., 2024) decompose neural activations into sparse, interpretable features. Circuit analysis (Olah et al., 2020; Olsson et al., 2022) investigates how these features compose into computational algorithms.

6.2. Sparse Dictionary Learning

Sparse dictionary learning has a rich history predating its application to mechanistic interpretability. K-SVD (Aharon et al., 2006) established foundational methods for learning overcomplete dictionaries, while theoretical work in compressed sensing (Donoho, 2006) characterized recovery conditions, with Spielman et al. (2012) providing polynomial-time algorithms for exact reconstruction under sparsity assumptions. Safran & Shamir (2018) demonstrated that spurious local minima are common even in simple two-layer ReLU networks, highlighting optimization challenges that persist in modern applications. Recent work has adapted these principles to mechanistic interpretability. SAEs (Cunningham et al., 2023) apply dictionary learning to language model activations. Various variants are further developed, including transcoders (Dunefsky et al., 2024), crosscoders (Gao et al., 2024), Matryoshka SAEs (Bussmann et al., 2025), and hybrid approaches like Language-Grounded Sparse Encoders (Tang et al., 2025a). These methods have found applications beyond language models, including protein structure analysis (Simon & Zou, 2024; Gujral et al., 2025), medical imaging (Abdulaal et al., 2024), model evaluation (Tang et al., 2025b), board game analysis (Karvonen et al., 2024), and fMRI data analysis Mao et al. (2025).

7. Conclusion

We propose the first unified theoretical framework for Sparse Dictionary Learning in mechanistic interpretability, and demonstrate how various SDL methods instantiate our framework. Under the Linear Representation Hypothesis with bounded feature interference, we established conditions for provable recovery of interpretable features and characterized the optimization landscape. We proved that spurious local minima correspond to feature absorption, providing the first theoretical explanation for the connection between feature absorption and local minima. To validate our theory, we designed the Linear Representation Bench, a benchmark that strictly instantiates our theoretical assumptions with fully accessible ground-truth features. Motivated by our theoretical findings and numerical experiments, we proposed feature anchoring, applicable for all SDL methods, and achieving improved feature recovery performance.

References

Abdulaal, A., Fry, H., Montaña-Brown, N., Ijishakin, A., Gao, J., Hyland, S., Alexander, D. C., and Castro, D. C. An x-ray is worth 15 features: Sparse autoencoders for interpretable radiology report generation, 2024. URL <https://arxiv.org/abs/2410.03334>.

Aharon, M., Elad, M., and Bruckstein, A. K-svd: An algorithm for designing overcomplete dictionaries for sparse

representation. *IEEE Transactions on signal processing*, 54(11):4311–4322, 2006.

Belinkov, Y. Probing classifiers: Promises, shortcomings, and advances, 2021. URL <https://arxiv.org/abs/2102.12452>.

Bereska, L. and Gavves, E. Mechanistic interpretability for ai safety – a review, 2024. URL <https://arxiv.org/abs/2404.14082>.

Bricken, T., Templeton, A., Batson, J., Chen, B., Jermyn, A., Conerly, T., Turner, N. L., Anil, C., Denison, C., Askell, A., Lasenby, R., Wu, Y., Kravec, S., Schiefer, N., Maxwell, T., Joseph, N., Tamkin, A., Nguyen, K., McLean, B., Burke, J. E., Hume, T., Carter, S., Henighan, T., and Olah, C. Towards monosemanticity: Decomposing language models with dictionary learning. *Transformer Circuits Thread*, 2023. URL <https://transformer-circuits.pub/2023/monosemantic-features>.

Bussmann, B., Leask, P., and Nanda, N. Batchtopk sparse autoencoders, 2024. URL <https://arxiv.org/abs/2412.06410>.

Bussmann, B., Nabeshima, N., Karvonen, A., and Nanda, N. Learning multi-level features with matryoshka sparse autoencoders, 2025. URL <https://arxiv.org/abs/2503.17547>.

Chanin, D., Wilken-Smith, J., Dulka, T., Bhatnagar, H., Golechha, S., and Bloom, J. A is for absorption: Studying feature splitting and absorption in sparse autoencoders, 2025. URL <https://arxiv.org/abs/2409.14507>.

Cui, J., Zhang, Q., Wang, Y., and Wang, Y. On the theoretical understanding of identifiable sparse autoencoders and beyond, 2025. URL <https://arxiv.org/abs/2506.15963>.

Cunningham, H., Ewart, A., Riggs, L., Huben, R., and Sharkey, L. Sparse autoencoders find highly interpretable features in language models, 2023. URL <https://arxiv.org/abs/2309.08600>.

Donoho, D. L. Compressed sensing. *IEEE Transactions on information theory*, 52(4):1289–1306, 2006.

Dunefsky, J., Chlenski, P., and Nanda, N. Transcoders find interpretable llm feature circuits, 2024. URL <https://arxiv.org/abs/2406.11944>.

Elhage, N., Hume, T., Olsson, C., Schiefer, N., Henighan, T., Kravec, S., Hatfield-Dodds, Z., Lasenby, R., Drain, D., Chen, C., Grosse, R., McCandlish, S., Kaplan, J., Amodei, D., Wattenberg, M., and Olah, C. Toy models

of superposition, 2022. URL <https://arxiv.org/abs/2209.10652>.

Gao, L., la Tour, T. D., Tillman, H., Goh, G., Troll, R., Radford, A., Sutskever, I., Leike, J., and Wu, J. Scaling and evaluating sparse autoencoders, 2024. URL <https://arxiv.org/abs/2406.04093>.

Gribonval, R. and Schnass, K. Dictionary identification - sparse matrix-factorisation via ℓ_1 -minimisation, 2010. URL <https://arxiv.org/abs/0904.4774>.

Gujral, O., Bafna, M., Alm, E., and Berger, B. Sparse autoencoders uncover biologically interpretable features in protein language model representations. *Proceedings of the National Academy of Sciences*, 122(34):e2506316122, 2025.

Jiang, Y., Rajendran, G., Ravikumar, P., Aragam, B., and Veitch, V. On the origins of linear representations in large language models, 2024. URL <https://arxiv.org/abs/2403.03867>.

Karvonen, A., Wright, B., Rager, C., Angell, R., Brinkmann, J., Smith, L., Verdun, C. M., Bau, D., and Marks, S. Measuring progress in dictionary learning for language model interpretability with board game models, 2024. URL <https://arxiv.org/abs/2408.00113>.

Koh, P. W., Nguyen, T., Tang, Y. S., Mussmann, S., Pierson, E., Kim, B., and Liang, P. Concept bottleneck models, 2020. URL <https://arxiv.org/abs/2007.04612>.

Lindsey, J., Templeton, A., Marcus, J., Conerly, T., Batson, J., and Olah, C. Sparse crosscoders for cross-layer features and model diffing. *Transformer Circuits Thread*, 2024. URL <https://transformer-circuits.pub/2024/crosscoders/index.html>.

Lipton, Z. C. The mythos of model interpretability, 2017. URL <https://arxiv.org/abs/1606.03490>.

Lundberg, S. and Lee, S.-I. A unified approach to interpreting model predictions, 2017. URL <https://arxiv.org/abs/1705.07874>.

Luo, Y., An, R., Zou, B., Tang, Y., Liu, J., and Zhang, S. Llm as dataset analyst: Subpopulation structure discovery with large language model, 2024. URL <https://arxiv.org/abs/2405.02363>.

Makhzani, A. and Frey, B. k-sparse autoencoders, 2014. URL <https://arxiv.org/abs/1312.5663>.

Mao, Z., Xu, J., Zheng, Z., Zheng, H., Sheng, D., Jin, Y., and Yang, G. Sparse autoencoders bridge the deep learning model and the brain, 2025. URL <https://arxiv.org/abs/2506.11123>.

Marks, S. and Tegmark, M. The geometry of truth: Emergent linear structure in large language model representations of true/false datasets, 2024. URL <https://arxiv.org/abs/2310.06824>.

Mienye, I. D. and Jere, N. A survey of decision trees: Concepts, algorithms, and applications. *IEEE access*, 12: 86716–86727, 2024.

Nanda, N., Lee, A., and Wattenberg, M. Emergent linear representations in world models of self-supervised sequence models, 2023. URL <https://arxiv.org/abs/2309.00941>.

Olah, C., Cammarata, N., Schubert, L., Goh, G., Petrov, M., and Carter, S. Zoom in: An introduction to circuits. *Distill*, 2020. doi: 10.23915/distill.00024.001. URL <https://distill.pub/2020/circuits/zoom-in/>.

Olsson, C., Elhage, N., Nanda, N., Joseph, N., DasSarma, N., Henighan, T., Mann, B., Askell, A., Bai, Y., Chen, A., Conerly, T., Drain, D., Ganguli, D., Hatfield-Dodds, Z., Hernandez, D., Johnston, S., Jones, A., Kernion, J., Lovitt, L., Ndousse, K., Amodei, D., Brown, T., Clark, J., Kaplan, J., McCandlish, S., and Olah, C. In-context learning and induction heads, 2022. URL <https://arxiv.org/abs/2209.11895>.

O’Neill, C. and Bui, T. Sparse autoencoders enable scalable and reliable circuit identification in language models, 2024. URL <https://arxiv.org/abs/2405.12522>.

Park, K., Choe, Y. J., and Veitch, V. The linear representation hypothesis and the geometry of large language models, 2024. URL <https://arxiv.org/abs/2311.03658>.

Park, K., Choe, Y. J., Jiang, Y., and Veitch, V. The geometry of categorical and hierarchical concepts in large language models, 2025. URL <https://arxiv.org/abs/2406.01506>.

Paulo, G., Shabalin, S., and Belrose, N. Transcoders beat sparse autoencoders for interpretability, 2025. URL <https://arxiv.org/abs/2501.18823>.

Quiroga, R. Q., Reddy, L., Kreiman, G., Koch, C., and Fried, I. Invariant visual representation by single neurons in the human brain. *Nature*, 435(7045):1102–1107, 2005.

Rajamanoharan, S., Conmy, A., Smith, L., Lieberum, T., Varma, V., Kramár, J., Shah, R., and Nanda, N. Improving dictionary learning with gated sparse autoencoders, 2024a. URL <https://arxiv.org/abs/2404.16014>.

Rajamanoharan, S., Lieberum, T., Sonnerat, N., Conmy, A., Varma, V., Kramár, J., and Nanda, N. Jumping ahead: Improving reconstruction fidelity with jumprelu sparse autoencoders, 2024b. URL <https://arxiv.org/abs/2407.14435>.

Rudin, C. Stop explaining black box machine learning models for high stakes decisions and use interpretable models instead, 2019. URL <https://arxiv.org/abs/1811.10154>.

Safran, I. and Shamir, O. Spurious local minima are common in two-layer relu neural networks, 2018. URL <https://arxiv.org/abs/1712.08968>.

Selvaraju, R. R., Cogswell, M., Das, A., Vedantam, R., Parikh, D., and Batra, D. Grad-cam: Visual explanations from deep networks via gradient-based localization. *International Journal of Computer Vision*, 128(2):336–359, October 2019. ISSN 1573-1405. doi: 10.1007/s11263-019-01228-7. URL <http://dx.doi.org/10.1007/s11263-019-01228-7>.

Sharkey, L., Chughtai, B., Batson, J., Lindsey, J., Wu, J., Bushnaq, L., Goldowsky-Dill, N., Heimersheim, S., Ortega, A., Bloom, J., Biderman, S., Garriga-Alonso, A., Conmy, A., Nanda, N., Rumbelow, J., Wattenberg, M., Schoots, N., Miller, J., Michaud, E. J., Casper, S., Tegmark, M., Saunders, W., Bau, D., Todd, E., Geiger, A., Geva, M., Hoogland, J., Murfet, D., and McGrath, T. Open problems in mechanistic interpretability, 2025. URL <https://arxiv.org/abs/2501.16496>.

Shu, D., Wu, X., Zhao, H., Rai, D., Yao, Z., Liu, N., and Du, M. A survey on sparse autoencoders: Interpreting the internal mechanisms of large language models, 2025. URL <https://arxiv.org/abs/2503.05613>.

Simon, E. and Zou, J. Interplm: Discovering interpretable features in protein language models via sparse autoencoders, 2024. URL <https://arxiv.org/abs/2412.12101>.

Spielman, D. A., Wang, H., and Wright, J. Exact recovery of sparsely-used dictionaries, 2012. URL <https://arxiv.org/abs/1206.5882>.

Sundararajan, M., Taly, A., and Yan, Q. Axiomatic attribution for deep networks, 2017. URL <https://arxiv.org/abs/1703.01365>.

Tang, Y., Lagzian, A., Anumasa, S., Zou, Q., Zhu, Y., Zhang, Y., Nguyen, T., Tham, Y.-C., Adeli, E., Cheng, C.-Y., Du, Y., and Liu, D. Human-like content analysis for generative ai with language-grounded sparse encoders, 2025a. URL <https://arxiv.org/abs/2508.18236>.

Tang, Y., Sinha, A., and Liu, D. How does my model fail? automatic identification and interpretation of physical plausibility failure modes with matryoshka transcoders, 2025b. URL <https://arxiv.org/abs/2511.10094>.

Templeton, A., Conerly, T., Marcus, J., Lindsey, J., Bricken, T., Chen, B., Pearce, A., Citro, C., Ameisen, E., Jones, A., Cunningham, H., Turner, N., McDougall, C., MacDiarmid, M., Freeman, C. D., Sumers, T. R., Rees, E., Batson, J., Jermyn, A., Carter, S., Olah, C., and Henighan, T. Scaling monosemanticity: Extracting interpretable features from claude 3 sonnet. *Transformer Circuits Thread*, 2024. URL <https://transformer-circuits.pub/2024/scaling-monosemanticity/>.

Vaswani, A., Shazeer, N., Parmar, N., Uszkoreit, J., Jones, L., Gomez, A. N., Kaiser, L., and Polosukhin, I. Attention is all you need, 2023. URL <https://arxiv.org/abs/1706.03762>.

Wang, M., la Tour, T. D., Watkins, O., Makelov, A., Chi, R. A., Miserendino, S., Wang, J., Rajaram, A., Heidecke, J., Patwardhan, T., and Mossing, D. Persona features control emergent misalignment, 2025. URL <https://arxiv.org/abs/2506.19823>.

A. Proof of Theorem 3.1

Proof. We establish how the loss decomposes when $S \rightarrow 1$. Let $W_r = [w_r^1, w_r^2, \dots, w_r^n]$ and $W_p = [w_p^1, w_p^2, \dots, w_p^n]$ denote the column representations of the reconstruction and projection matrices.

Under extreme sparsity ($S \rightarrow 1$), we consider at most one component $x_d(s)$ is active for any given input, and consider other scenarios as of low probability. The expectation decomposes over activation patterns:

$$\mathcal{L}_{\text{SDL}} = \mathbb{E}_s \|W_r \mathbf{x}(s) - W_d \sigma(W_e W_p \mathbf{x}(s))\|^2 \quad (23)$$

$$= \sum_{m=0}^n \Pr(\|\mathbf{x}(s)\|_0 = m) \cdot \mathbb{E}[\|\mathbf{x}_r(s) - W_d \sigma(W_e \mathbf{x}_p(s))\|^2 \mid \|\mathbf{x}(s)\|_0 = m] \quad (24)$$

$$= \Pr(\|\mathbf{x}(s)\|_0 = 0) \cdot 0 \quad (25)$$

$$+ \sum_{d=1}^n \Pr(\mathbf{x}(s) = x_d(s) \mathbf{e}_d) \cdot \mathbb{E}_{x_d(s)} \left[x_d(s)^2 \|w_r^d - W_d \sigma(W_e w_p^d)\|^2 \mid x_d(s) > 0 \right] \quad (26)$$

$$+ \sum_{m=2}^n \Pr(\|\mathbf{x}(s)\|_0 = m) \cdot \mathbb{E}[\|\mathbf{x}_r(s) - W_d \sigma(W_e \mathbf{x}_p(s))\|^2 \mid \|\mathbf{x}(s)\|_0 = m] \quad (27)$$

$$= \sum_{d=1}^n M_d \|w_r^d - W_d \sigma(W_e w_p^d)\|^2 + O((1-S)^2) \quad (28)$$

□

B. Proof of Theorem 3.2

Proof. We analyze the approximate loss $\tilde{\mathcal{L}}_{\text{SDL}}(W_d^*, W_e^*)$ by examining the reconstruction error for each ground-truth feature when active in isolation.

Consider feature $d \in [n]$ active in isolation. The encoder output is $W_e^* w_p^d = W_p^\top w_p^d$ with k -th component:

$$(W_e^* w_p^d)_k = \langle w_p^k, w_p^d \rangle \quad (29)$$

Under Assumption 2.4, the unit-norm condition gives $(W_e^* w_p^d)_d = 1$. For $k \neq d$, the bounded interference condition implies $\langle w_p^k, w_p^d \rangle \leq M$, where M is the maximum interference. Combined with the Cauchy-Schwarz inequality, we have:

$$\langle w_p^k, w_p^d \rangle \in [-1, M] \quad \forall k \neq d \quad (30)$$

Define the set of activated neurons for feature d :

$$\mathcal{A}_d = \{k \in [n] : \sigma(W_e^* w_p^d)_k > 0\} \quad (31)$$

Since $\sigma(z)_i \in \{0, z_i\}$ and typical activation functions satisfy $\sigma(z)_i > 0 \iff z_i > c$ for some threshold $c \geq 0$, we have:

$$\mathcal{A}_d = \{k \in [n] : \langle w_p^k, w_p^d \rangle > c\} \quad (32)$$

Note that $d \in \mathcal{A}_d$ since $(W_e^* w_p^d)_d = 1 > c \geq 0$. For $k \neq d$, neuron k activates only if $\langle w_p^k, w_p^d \rangle > c \geq 0$, which requires positive interference. Therefore:

$$\mathcal{A}_d \setminus \{d\} \subseteq \{k \in [n] : 0 < \langle w_p^k, w_p^d \rangle \leq M\} \quad (33)$$

Let $K_d = |\mathcal{A}_d|$ denote the number of activated neurons.

The activation output satisfies $\sigma(W_e^* w_p^d)_k = \langle w_p^k, w_p^d \rangle$ for $k \in \mathcal{A}_d$ and zero otherwise, since $\sigma(z)_i \in \{0, z_i\}$. The

reconstruction is therefore $W_d^* \sigma(W_e^* w_p^d) = \sum_{k \in \mathcal{A}_d} \langle w_p^k, w_p^d \rangle w_r^k$. The reconstruction error for feature d is

$$w_r^d - W_d^* \sigma(W_e^* w_p^d) = w_r^d - \sum_{k \in \mathcal{A}_d} \langle w_p^k, w_p^d \rangle w_r^k \quad (34)$$

$$= w_r^d - w_r^d - \sum_{k \in \mathcal{A}_d \setminus \{d\}} \langle w_p^k, w_p^d \rangle w_r^k \quad (35)$$

$$= - \sum_{k \in \mathcal{A}_d \setminus \{d\}} \langle w_p^k, w_p^d \rangle w_r^k \quad (36)$$

Under the unit-norm assumption, $\|w_r^k\| = 1$ for all k . For $k \in \mathcal{A}_d \setminus \{d\}$, we have $\langle w_p^k, w_p^d \rangle > 0$ (since negative interference does not activate) and $\langle w_p^k, w_p^d \rangle \leq M$ by the bounded interference condition. Therefore, using the triangle inequality:

$$\|w_r^d - W_d^* \sigma(W_e^* w_p^d)\| \leq \sum_{k \in \mathcal{A}_d \setminus \{d\}} |\langle w_p^k, w_p^d \rangle| \cdot \|w_r^k\| \quad (37)$$

$$= \sum_{k \in \mathcal{A}_d \setminus \{d\}} \langle w_p^k, w_p^d \rangle \cdot 1 \quad (\text{positive terms}) \quad (38)$$

$$\leq \sum_{k \in \mathcal{A}_d \setminus \{d\}} M \quad (39)$$

$$= M(K_d - 1) \quad (40)$$

Squaring both sides: $\|w_r^d - W_d^* \sigma(W_e^* w_p^d)\|^2 \leq M^2(K_d - 1)^2$. The approximate loss is

$$\tilde{\mathcal{L}}_{\text{SDL}}(W_d^*, W_e^*) = \sum_{d=1}^n M_d \cdot M^2(K_d - 1)^2 \leq M^2 \sum_{d=1}^n M_d(K_d - 1)^2 \quad (41)$$

Since $K_d \geq 1$ for all d and typically $K_d = O(1)$ for most features (as the activation function provides sparsity), we have $(K_d - 1)^2 = O(1)$. Under the feature independence and stability assumptions (Assumption 2.4), $\sum_{d=1}^n M_d = \sum_{d=1}^n \Pr(\mathbf{x}(s) = x_d(s)e_d) \cdot \mathbb{E}[x_d(s)^2 | x_d(s) > 0] = O(1 - S)$, since the probability that exactly one feature is active is $(1 - S)$ under extreme sparsity. Therefore:

$$\tilde{\mathcal{L}}_{\text{SDL}}(W_d^*, W_e^*) = O(M^2(1 - S)) \quad (42)$$

This completes the proof. \square

C. Proof of Theorem 3.5

Proof. We construct a point (W_d, W_e) exhibiting the polysemanticity pattern and verify it satisfies all three conditions.

Step 1: Construction of encoder W_e . Given a realizable polysemanticity pattern $(\mathcal{F}_1, \dots, \mathcal{F}_{n_q})$, by Definition ??, there exists an encoder $W_e = [(w_e^1)^\top, \dots, (w_e^{n_q})^\top]^\top$ such that for all $i \in [n_q]$:

$$\mathcal{F}_i = \left\{ d \in [n] : (\sigma(W_e w_p^d))_i > 0 \right\}. \quad (43)$$

Fix this W_e for the remainder of the proof. Define the activation vectors:

$$z_d := \sigma(W_e w_p^d) \in \mathbb{R}^{n_q}, \quad d = 1, \dots, n. \quad (44)$$

By construction, $(z_d)_i > 0$ if and only if $d \in \mathcal{F}_i$.

Partition the neurons into active and dead sets:

$$\mathcal{A} = \{i \in [n_q] : \mathcal{F}_i \neq \emptyset\}, \quad \mathcal{D} = \{i \in [n_q] : \mathcal{F}_i = \emptyset\}. \quad (45)$$

Step 2: Gradient analysis with respect to W_d . The gradient of the loss with respect to the i -th decoder column $w_d^i \in \mathbb{R}^{n_r}$ is:

$$\nabla_{w_d^i} \tilde{\mathcal{L}}_{\text{SDL}} = -2 \sum_{d=1}^n M_d (w_r^d - W_d z_d) (z_d)_i. \quad (46)$$

Case 1: Dead neurons ($i \in \mathcal{D}$). For $i \in \mathcal{D}$, we have $\mathcal{F}_i = \emptyset$, which implies $(z_d)_i = 0$ for all $d \in [n]$. Therefore:

$$\nabla_{w_d^i} \tilde{\mathcal{L}}_{\text{SDL}} = 0 \quad \forall w_d^i. \quad (47)$$

The decoder weights for dead neurons are arbitrary. We set $w_d^i = 0$ for all $i \in \mathcal{D}$.

Case 2: Active neurons ($i \in \mathcal{A}$). For $i \in \mathcal{A}$, we have $\mathcal{F}_i \neq \emptyset$. The gradient vanishes when:

$$\sum_{d \in \mathcal{F}_i} M_d w_r^d (z_d)_i = \sum_{d \in \mathcal{F}_i} M_d (W_d z_d) (z_d)_i. \quad (48)$$

Expanding the right side and using the fact that $(z_d)_j = 0$ for $j \notin \mathcal{F}_j$ or $d \notin \mathcal{F}_j$:

$$\sum_{d \in \mathcal{F}_i} M_d w_r^d (z_d)_i = \sum_{j=1}^{n_q} w_d^j \underbrace{\sum_{d \in \mathcal{F}_i \cap \mathcal{F}_j} M_d (z_d)_i (z_d)_j}_{=: A_{ij}}. \quad (49)$$

Define the Gram matrix $A \in \mathbb{R}^{n_q \times n_q}$:

$$A_{ij} = \sum_{d \in \mathcal{F}_i \cap \mathcal{F}_j} M_d (z_d)_i (z_d)_j. \quad (50)$$

And the target matrix $B \in \mathbb{R}^{n_r \times n_q}$:

$$B_{:,i} = \sum_{d \in \mathcal{F}_i} M_d w_r^d (z_d)_i. \quad (51)$$

The stationarity condition becomes:

$$B = W_d A. \quad (52)$$

Step 3: Properties of the Gram matrix A .

Claim 3.1: Block structure. The matrix A has a block-diagonal structure with respect to the partition $(\mathcal{A}, \mathcal{D})$:

$$A = \begin{bmatrix} A_{\mathcal{A}\mathcal{A}} & 0 \\ 0 & 0 \end{bmatrix}, \quad (53)$$

where $A_{\mathcal{A}\mathcal{A}}$ corresponds to rows and columns indexed by \mathcal{A} .

Proof of Claim 3.1: For $i \in \mathcal{D}$, we have $\mathcal{F}_i = \emptyset$, so $\mathcal{F}_i \cap \mathcal{F}_j = \emptyset$ for all j , giving $A_{ij} = 0$. Similarly, $A_{ji} = 0$. For $i, j \in \mathcal{A}$, $A_{ij} = 0$. \square

Claim 3.2: Positive definiteness. The submatrix $A_{\mathcal{A}\mathcal{A}}$ is positive definite.

Proof of Claim 3.2: For any nonzero $v \in \mathbb{R}^{|\mathcal{A}|}$, consider:

$$v^\top A_{\mathcal{A}\mathcal{A}} v = \sum_{i,j \in \mathcal{A}} v_i v_j A_{ij} \quad (54)$$

$$= \sum_{i,j \in \mathcal{A}} v_i v_j \sum_{d \in \mathcal{F}_i \cap \mathcal{F}_j} M_d (z_d)_i (z_d)_j \quad (55)$$

$$= \sum_{d=1}^n M_d \left(\sum_{i \in \mathcal{A}: d \in \mathcal{F}_i} v_i (z_d)_i \right)^2. \quad (56)$$

Since $(\mathcal{F}_1, \dots, \mathcal{F}_{n_q})$ forms a partition of $[n]$, for each $d \in [n]$, there exists at least one $i \in \mathcal{A}$ with $d \in \mathcal{F}_i$ and $(z_d)_i > 0$. For any nonzero v , at least one term in the sum is positive, giving $v^\top A_{\mathcal{A}\mathcal{A}} v > 0$. \square

Step 4: Optimal decoder solution. From the normal equations (52), the optimal decoder for active neurons is:

$$W_d^*[:, \mathcal{A}] = B[:, \mathcal{A}] (A_{\mathcal{A}\mathcal{A}})^{-1}, \quad (57)$$

where $(A_{\mathcal{A}\mathcal{A}})^{-1}$ exists by Claim 3.2. For dead neurons, we set:

$$W_d^*[:, \mathcal{D}] = 0. \quad (58)$$

This gives $\nabla_{W_d} \tilde{\mathcal{L}}_{\text{SDL}}(W_d^*, W_e) = 0$, proving condition (2).

Step 5: Hessian analysis. The Hessian with respect to W_d has Kronecker structure:

$$\nabla_{W_d}^2 \tilde{\mathcal{L}}_{\text{SDL}} = I_{n_r} \otimes (2A). \quad (59)$$

For positive semi-definiteness, we need to show $A \succeq 0$. From the block structure (Claim 3.1) and positive definiteness of $A_{\mathcal{A}\mathcal{A}}$ (Claim 3.2):

$$A = \begin{bmatrix} A_{\mathcal{A}\mathcal{A}} & 0 \\ 0 & 0 \end{bmatrix} \succeq 0, \quad (60)$$

which implies $\nabla_{W_d}^2 \tilde{\mathcal{L}}_{\text{SDL}}(W_d^*, W_e) \succeq 0$, proving condition (3).

Step 6: Non-zero loss for polysemantic patterns. We now prove that $\tilde{\mathcal{L}}_{\text{SDL}}(W_d^*, W_e) > 0$ when the pattern exhibits polysemanticity.

By Theorem ??, $\tilde{\mathcal{L}}_{\text{SDL}} = 0$ if and only if:

$$w_r^d = W_d \sigma(W_e w_p^d) = W_d z_d \quad \forall d \in [n]. \quad (61)$$

Since the pattern has at least one $|\mathcal{F}_i| \geq 2$, fix such an $i \in \mathcal{A}$ and choose $d_1, d_2 \in \mathcal{F}_i$ with $d_1 \neq d_2$. Both features activate neuron i , so $(z_{d_1})_i > 0$ and $(z_{d_2})_i > 0$.

The perfect reconstruction conditions for these features are:

$$w_r^{d_1} = \sum_{j=1}^{n_q} w_d^j (z_{d_1})_j = \sum_{j \in \mathcal{F}_j: d_1 \in \mathcal{F}_j} w_d^j (z_{d_1})_j, \quad (62)$$

$$w_r^{d_2} = \sum_{j=1}^{n_q} w_d^j (z_{d_2})_j = \sum_{j \in \mathcal{F}_j: d_2 \in \mathcal{F}_j} w_d^j (z_{d_2})_j. \quad (63)$$

Both sums include the term $w_d^i (z_{d_k})_i$ for $k \in \{1, 2\}$. However, the coefficients differ: $(z_{d_1})_i \neq (z_{d_2})_i$ in general (since different input patterns).

Key observation: Under Assumption 2.4, $w_r^{d_1} \not\propto w_r^{d_2}$ for distinct features. If both (61) equations held, we would need:

$$\frac{w_r^{d_1}}{(z_{d_1})_i} = w_d^i = \frac{w_r^{d_2}}{(z_{d_2})_i}, \quad (64)$$

which requires $w_r^{d_1} \propto w_r^{d_2}$, contradicting Assumption 2.4.

Therefore, the optimal decoder W_d^* cannot satisfy (61) for all d , giving:

$$\tilde{\mathcal{L}}_{\text{SDL}}(W_d^*, W_e) = \sum_{d=1}^n M_d \|w_r^d - W_d^* z_d\|^2 > 0, \quad (65)$$

proving condition (1).

Conclusion. We have constructed (W_d^*, W_e) exhibiting the polysemanticity pattern such that all three conditions hold, completing the proof. \square

D. Proof of Theorem 3.8

Proof. We show that hierarchical concept structures naturally give rise to polysemy patterns with feature absorption, and then apply Theorem 3.5 to establish the existence of local minima.

Consider ground-truth features exhibiting hierarchical structure with parent concept p and sub-concepts $\mathcal{C} = \{c_1, \dots, c_k\}$ satisfying Definition 3.7. Any partition of \mathcal{C} into non-empty subsets $\mathcal{C}_1, \mathcal{C}_2$ with $\mathcal{C}_1 \cup \mathcal{C}_2 = \mathcal{C}$ and $\mathcal{C}_1 \cap \mathcal{C}_2 = \emptyset$ induces a polysemy pattern as follows.

Define $(\mathcal{F}_1, \dots, \mathcal{F}_{n_q})$ where:

- $\mathcal{F}_i = \mathcal{C}_1$ for some neuron $i \in [n_q]$
- $\mathcal{F}_j = \mathcal{C}_2$ for some neuron $j \in [n_q], j \neq i$
- $\mathcal{F}_\ell = \emptyset$ for all other neurons $\ell \notin \{i, j\}$

This constitutes a polysemy pattern since:

1. $(\mathcal{F}_1, \dots, \mathcal{F}_{n_q})$ forms a partition of $[n]$ restricted to the sub-concepts (assuming other ground-truth features are assigned to other neurons)
2. At least one of $|\mathcal{F}_i| \geq 2$ or $|\mathcal{F}_j| \geq 2$ holds, satisfying the polysemy condition in Definition 3.4
3. The pattern exhibits feature absorption: neuron i captures a subset of sub-concepts (absorbed feature) while neuron j captures the remaining sub-concepts (main line interpretation)

If this polysemy pattern is realizable (Definition 3.4), then by Theorem 3.5, there exists a configuration (W_d, W_e) that is a local minimum of $\tilde{\mathcal{L}}_{SDL}$ exhibiting this pattern. This completes the proof. \square

E. The Linear Representation Bench

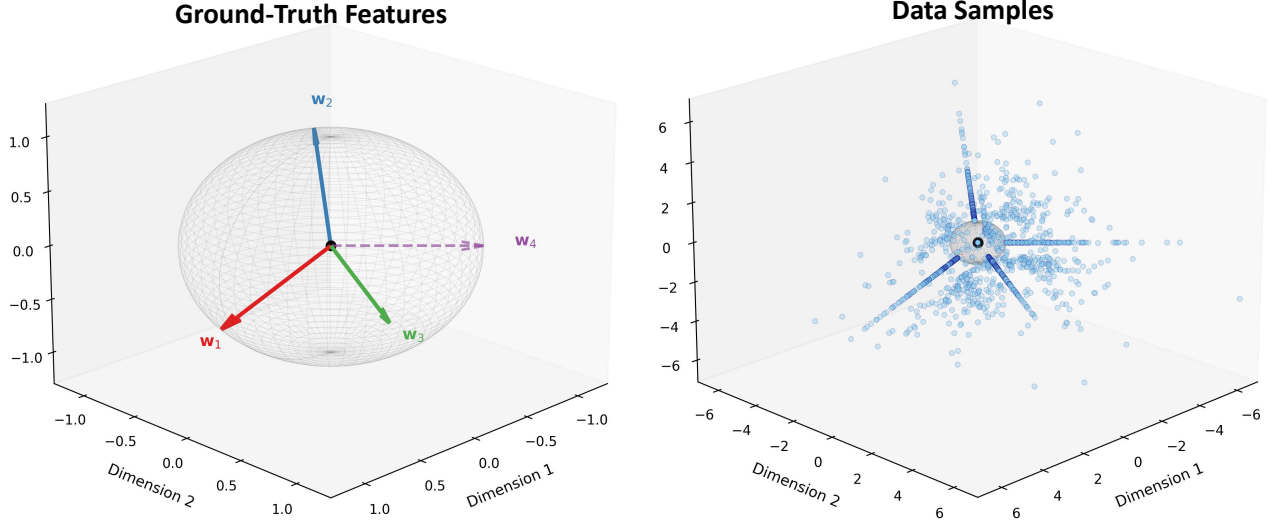


Figure 8. Visualization of the Linear Representation Bench. The figure illustrates a $D = 3$ dimensional representation space generated using $N = 4$ feature directions (\mathbf{W}_p).

F. Limitations and Future Works

While our theoretical framework provides valuable insights into SDL methods, several limitations warrant discussion:

- **Assumption Violations.** Our analysis relies on Assumptions 2.3 and 2.4, which may not hold perfectly in realworld neural networks.
- **Extreme Sparsity.** Some of our theoretical results are limited to the extreme sparsity ($S \rightarrow 1$) assumption, which may not hold in realworld neural networks.
- **Convergence Guarantees.** We characterize the global and local minima of the optimization landscape. Future works can provide convergence guarantees or sample complexity bounds following our framework.
- **Classical SDL Methods.** Established dictionary learning algorithms have demonstrated success in signal processing but remain unexplored for mechanistic interpretability, representing promising future directions.